Stable Emulsions Formed by Self-Assembly of Interfacial Networks of Dipeptide Derivatives

Shuo Bai,[†,§,*] Charalampos Pappas,[†,§] Sisir Debnath,[†] Pim W. J. M. Frederix,[†] Joy Leckie,[†] Scott Fleming,[†] and Rein V. Ulijn[†,‡,*]

[†]WestCHEM, Department of Pure and Applied Chemistry, University of Strathclyde, Glasgow G1 1XL, U.K. and [‡]Advanced Science Research Center (ASRC), City University of New York, New York, New York 10031, United States. [§]S. Bai and C. Pappas contributed equally.

ABSTRACT We demonstrate the use of dipeptide amphiphiles that, by hand shaking of a biphasic solvent system for a few seconds, form emulsions that remain stable for months through the formation of nanofibrous networks at the organic/aqueous interface. Unlike absorption of traditional surfactants, the interfacial networks form by self-assembly through π-stacking interactions and hydrogen bonding. Altering the dipeptide sequence has a dramatic effect on the properties of the emulsions formed, illustrating the possibility of tuning emulsion properties by chemical design. The systems provide superior long-term stability toward temperature and salts compared to with sodium dodecyl sulfate (SDS) and can be enzymatically disassembled causing on-demand demulsification under mild conditions. The interfacial networks facilitate highly tunable and stable encapsulation and compartmentalization with potential applications in cosmetics, therapeutics, and food industry.

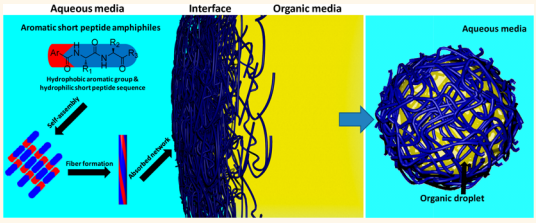

KEYWORDS: dipeptide · self-assembly · emulsion · interface · microcapsules

Surfactant-based emulsions for encapsulation and phase separation have been extensively utilized in food, cosmetics, coating, catalysis, encapsulation, drug delivery and cell assays.[1−10] Development of new interfacial stabilization strategies is the key to the advancement of next generation emulsification technologies. Traditional surfactants have disadvantages including toxicity, limited stability toward temperature, pH and salts.[11,12] A number of approaches, using biocompatible copolymers,[13−18] lipids[19] and polypeptides[20−23] as novel surfactants, biomacromolecules and proteins that form networked films[24,25] or Pickering emulsion based on solid particles[26−32] and polymersomes,[33−36] have been developed to complement traditional emulsion systems.

Self-assembling small molecules are increasingly investigated as alternatives to polymers as structured materials and gels with advantages such as stimuli-responsiveness biocompatibility, *etc.* In particular, self-assembly of aromatic peptide amphiphiles, containing a hydrophilic short (di- or tri-) peptide sequence with the N-terminus capped by a hydrophobic synthetic aromatic moiety, are versatile building blocks for the production, *via* molecular self-assembly, of nanostructures with a variety of morphologies and properties,[37−40] including localized assembly at solid/liquid interfaces[41−44] and in microdroplets.[45−47]

Aromatic peptide amphiphiles have not yet been used to produce interfacial networks to stabilize emulsions. Thus, as an alternative to emulsion stabilization by absorption of surfactants, we demonstrate nanostructured networks at interfaces as versatile emulsion stabilizing systems. The approach combines tunable properties, through molecular design by taking advantage of a balance between intermolecular aromatic π-stacking and hydrogen bond interactions,[48−52] with long-term high stability at elevated temperature and in the presence of salts when compared with traditional surfactant sodium dodecyl sulfate (SDS), and controllable breaking of emulsions by enzymatic hydrolysis.[53]

RESULTS AND DISCUSSION

In this work, we demonstrate a series of aromatic short peptide amphiphiles by

* Address correspondence to shuo.bai@strath.ac.uk, rein.ulijn@strath.ac.uk.

Received for review April 7, 2014 and accepted June 4, 2014.

Published online June 04, 2014
10.1021/nn501909j

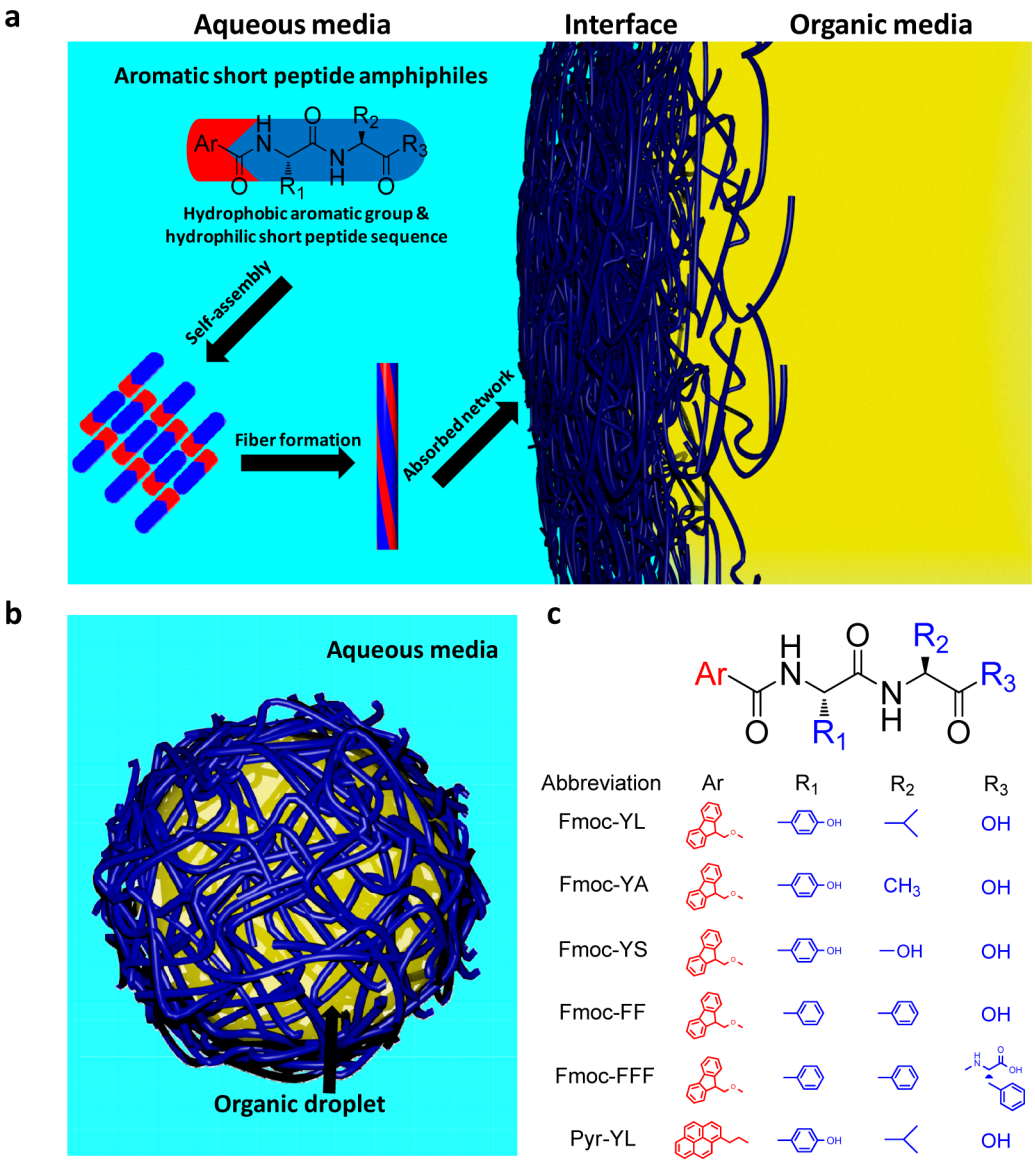

Scheme 1. (a) Cartoon of self-assembly and formation of fibrous network of aromatic short peptide amphiphiles at oil/water interface. (b) Cartoon of oil-in-water droplets stabilized by peptide fibrous network. (c) Chemical structure of aromatic peptide derivatives including Fmoc-YL, Fmoc-YA, Fmoc-YS, Fmoc-FF, Fmoc-FFF and Pyrene-YL.

combining 9-fluorenylmethoxycarbonyl (Fmoc) or pyrene (Pyr) with di- or tri- peptides tyrosine-leucine (YL), tyrosine-alanine (YA), tyrosine-serine (YS), diphenylalanine (FF) and triphenylalanine (FFF) with varying hydrophobicity and functional groups (Scheme 1) that self-assemble at the organic/aqueous interfaces rapidly forming highly stable microcapsules fibrous network. Unlike absorption of traditional surfactants with hydrophilic head and hydrophobic tail at interfaces, the nanostructures self-assembled by aromatic $\pi-\pi$ stacking and hydrogen bonding of peptide sequences to stabilize the organic (or water) droplets in aqueous (or organic) media (Scheme 1b).

Our interest in studying aromatic peptide amphiphiles at the organic/aqueous interface started from the discovery that aromatic peptide Fmoc-YL forms gel in both phosphate buffer solution (10 mM) and chloroform (25 mM) (Figure S1, Supporting Information). At low concentrations Fmoc-YL (0.5 mM) was shown to transfer between aqueous and organic phases to reach an equilibrium distribution.[54,55] By adding different volumes of chloroform to 10 mM Fmoc-YL buffer solution at 80 °C (the volume ratio of buffer solution to chloroform is altered from 1:9, 3:7, 5:5, 7:3, to 9:1), after manual agitation for 5 s emulsions form in vials, as Figure 1a shown. These remain stable for months, showing that the formed peptide layers provide an excellent barrier to prevent coalescence. In the images shown, the milky layers are emulsions and the transparent layers above and below are aqueous and chloroform phase, respectively. UV—vis was used to determine the amount of Fmoc-YL that remained in water phase and transferred to chloroform as Figure S2 (Supporting Information)

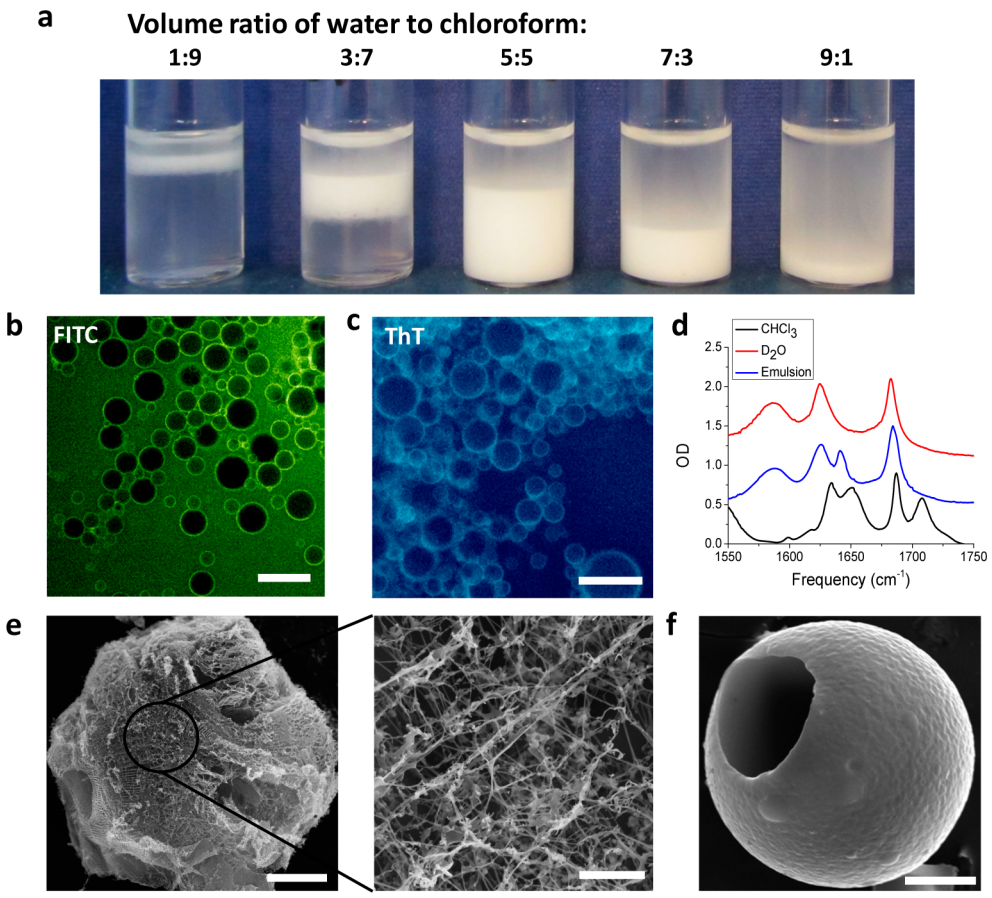

Figure 1. (a) Optical photographs of glass vials in which chloroform-in-water emulsions (white foamy layer) were prepared by adding 10 mmol·L^{-1} Fmoc-YL phosphate buffer solution (pH 8) to chloroform with manual agitation. From left to right, the volume ratio of buffer solution to chloroform is altered from 1:9, 3:7, 5:5, 7:3, to 9:1, and samples are named as W1C9, W3C7, W5C5, W7C3 and W9C1. (b) Fluorescent microscope image of chloroform-in-water emulsion droplets stabilized by Fmoc-YL networks containing FITC in water phase (Sample W3C7). Scale bar is 50 μm. (c) Fluorescent microscope image of chloroform-in-water emulsion droplets stabilized by ThT labeled Fmoc-YL networks (Sample W3C7). Scale bar is 50 μm. (d) FTIR spectra of self-assembly of Fmoc-YL in chloroform (black), D_2O phosphate buffer solution (pH 8) (red) and at interfaces stabilizing emulsions (blue). (e) SEM micrographs of Fmoc-YL networks at chloroform/water interface stabilizing the chloroform-in-water emulsions. The samples are prepared at freeze-drying condition. The scale bars are 50 μm (left) and 2 μm (right). (f) SEM micrograph of Fmoc-YL microcapsules at chloroform/water interface. The sample is prepared at air-drying condition and scale bar is 2 μm.

shown. Fluorescein isothiocyanate (FITC) was used to label the aqueous phase in the emulsion layers for imaging by fluorescence microscopy. Figure 1b and S3a (Supporting Information) indicate that chloroform-in-water emulsions form after emulsification stabilized by Fmoc-YL.

The absorption of Fmoc-YL at the chloroform/water interfaces could be quantified by UV−vis spectra by measuring the concentration in each phase and with the remainder absorbed at the interface. On the basis of UV analysis, shown in Figure S4a (Supporting Information), in a 50:50 water/chloroform system, the amount of Fmoc-YL absorbed at the chloroform/water interface could be calculated as 1.9 mmol·m^{-2}. Figure S4b (Supporting Information) shows that the calculated maximum absorption of a close-packed monolayer of Fmoc-YL is 3.4 μmol·m^{-2} indicating that Fmoc-YL absorbed at the interfaces is composed of a film rather than a monolayer.

Next, we investigated the structure of this peptide interfacial film at the chloroform/water interface, using a range of microscopy and spectroscopy technologies. Thioflavin T (ThT) was used to label self-assembled peptide structures.[56] Figure S5 (Supporting Information) shows the labeling of Fmoc-YL nanofibrous gels by ThT in water and chloroform. After dissolving the Fmoc-YL with ThT in both solvents, there is low emission in water and almost no emission in chloroform is observed, while upon gelation (24 h) the appearance of stronger emission in both water and chloroform demonstrates that the self-assembled β sheet-like of fibrous structures are formed. ThT was subsequently used to label the interfacial film, Figure 1c and S3b (Supporting Information) show that a Fmoc-YL shell stabilized the organic droplets suggesting the self-assembly of peptide β sheet-like structures at the interface.

Infrared spectroscopy was then used to determine the H-bonding interactions that underpin self-assembly

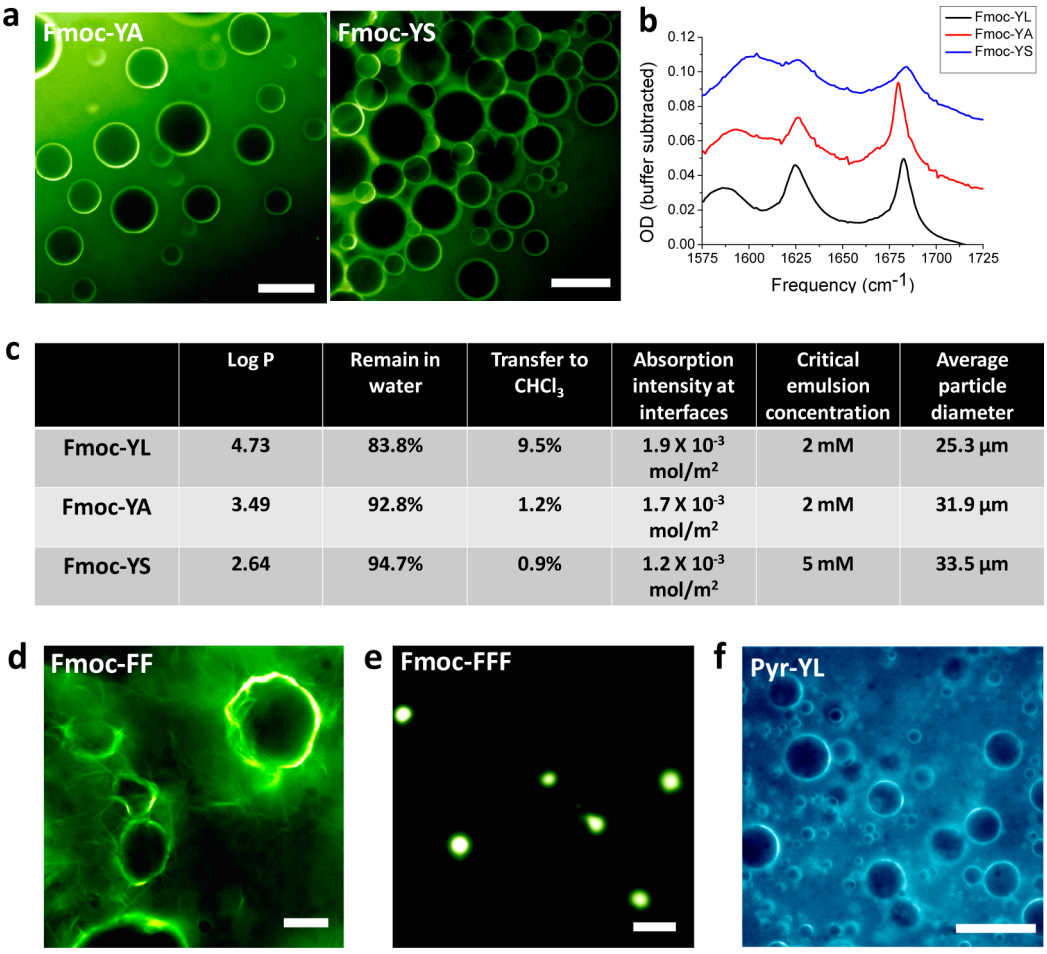

c

	Log P	Remain in water	Transfer to $CHCl_3$	Absorption intensity at interfaces	Critical emulsion concentration	Average particle diameter
Fmoc-YL	4.73	83.8%	9.5%	1.9 X 10^{-3} mol/m^2	2 mM	25.3 μm
Fmoc-YA	3.49	92.8%	1.2%	1.7 X 10^{-3} mol/m^2	2 mM	31.9 μm
Fmoc-YS	2.64	94.7%	0.9%	1.2 X 10^{-3} mol/m^2	5 mM	33.5 μm

Figure 2. (a) Fluorescent microscope images of chloroform-in-water emulsion droplets stabilized by Fmoc-YA (left) and Fmoc-YS (right) networks containing FITC in water phase. Scale bar is 50 μm. (b) FTIR spectra of 10 mmol·L^{-1} Fmoc-YL, Fmoc-YA and Fmoc-YS in D_2O phosphate buffer solution (pH 8). (c) Table of the calculated partition coefficient (log P) and the measured partitioning of peptides between water, chloroform and accumulated at the interface, the critical emulsion concentration (obtained from emulsification experiments as Figure S8, Supporting Information, shown) of Fmoc-YL, Fmoc-YA and Fmoc-YS and the average diameters of emulsions droplets. Fluorescent microscope images of (d) chloroform-in-water emulsion droplets stabilized by Fmoc-FF containing FITC in water phase, (e) water-in-chloroform emulsion droplets stabilized by Fmoc-FFF containing FITC in water phase and (f) chloroform-in-water emulsion droplets stabilized by Pyrene-YL. Scale bar is 50 μm.

of Fmoc-YL fibrous structure in water, chloroform and at the interface. Figure 1d shows an infrared absorption spectrum in D_2O typical for peptides in a well-ordered β sheet-like arrangement with peaks at 1623 and 1684 cm^{-1} for amide and carbamate moieties, respectively.[57] In chloroform, these peaks were observed at 1632 and 1687 cm^{-1} with an additional absorption at 1652 cm^{-1} indicating the presence of a less-ordered H-bonding network. Additionally, a peak assigned to the carboxylate group of the C-terminus was found at 1588 cm^{-1} in water, while a peak was observed at 1708 cm^{-1} in chloroform indicating protonation of the C-terminus in the organic solvent. At the interface, Fmoc-YL adopts a confirmation that is similar to the chloroform system with two peaks, indicating a less ordered β sheet-like environment (1623 and 1641 cm^{-1}). The C termini remain (in part) deprotonated as indicated by a peak at (1588 cm^{-1}) suggesting that the nanostructured network is predominantly situated in the aqueous phase.

Scanning electron microscope (SEM) was used to visualize the interfacial Fmoc-YL film. Freeze-drying was used to prepare the samples with retention of structure. Figure 1e shows fibrous networks at the interface. Upon air-drying condition, Figure 1f and S6a (Supporting Information) show the peptide stabilized emulsion droplets that remain as microcapsules after solvent evaporation and consequent shrinking.

The properties of aromatic peptide amphiphiles, such as hydrophobicity and chemical groups which may affect the emulsification, can be altered by changing the aromatic group or peptide sequence. We prepared a series of peptide amphiphiles by changing one amino acid on the peptide sequence with decreasing hydrophobicity from tyrosine-leucine (YL), tyrosine-alanine (YA) to tyrosine-serine (YS). Fmoc-YA can form gel in both buffer solution and chloroform (30 mM), while Fmoc-YS only forms gel in aqueous media under

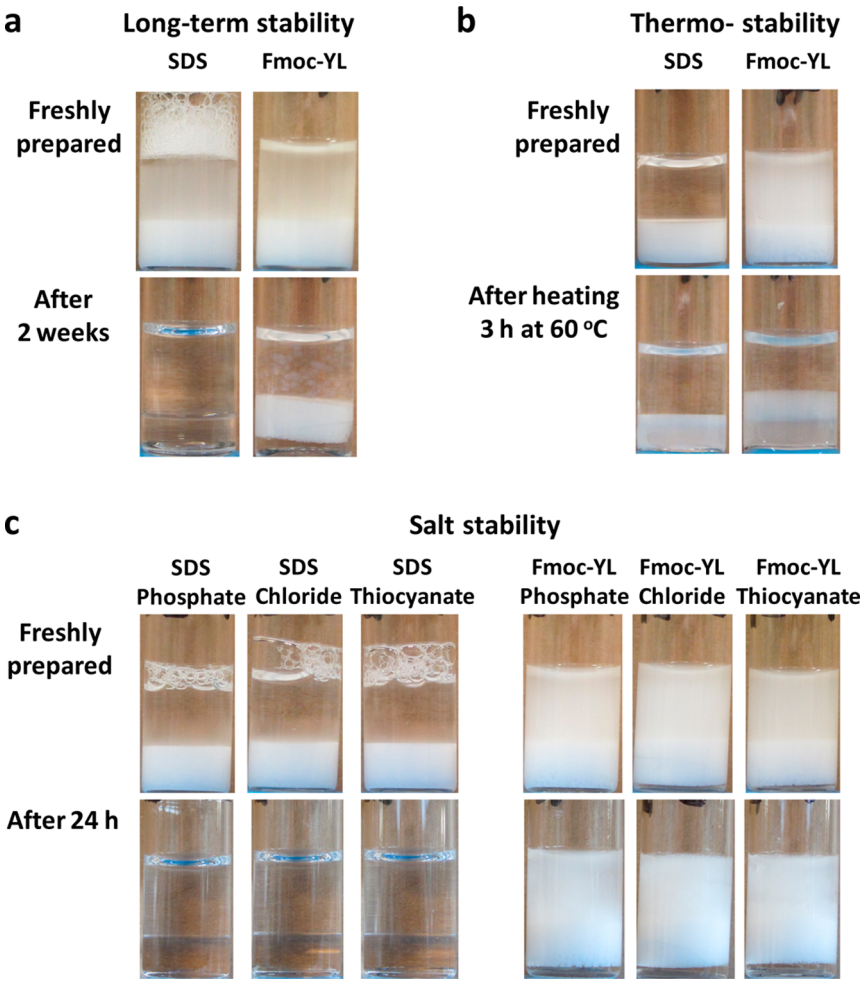

Figure 3. (a) Optical photographs of glass vials in which chloroform-in-water emulsions (white foamy layer) were prepared with 10 mmol·L^{-1} SDS solution and Fmoc-YL phosphate buffer solution by manual agitation. The top images show freshly prepared emulsions, and the bottom images show emulsions incubated for 2 weeks. (b) Optical photographs of glass vials in which chloroform-in-water emulsions (white foamy layer) were prepared with 10 mmol·L^{-1} SDS solution and Fmoc-YL phosphate buffer solution by manual agitation. The top images show freshly prepared emulsions, and the bottom images show emulsions heated at 60 °C for 3 h. (c) Optical photographs of glass vials in which chloroform-in-water emulsions (white foamy layer) were prepared with 10 mmol·L^{-1} SDS and Fmoc-YL in 100 mM phosphate, chloride and thiocyanate buffer solution by manual agitation. The top images show freshly prepared emulsions, and the bottom images show emulsions incubated for 24 h.

these conditions. Atomic force microscopy (AFM) images (Figure S7, Supporting Information) show the formation of fibrous structure of Fmoc-YL, Fmoc-YA and Fmoc-YS gels in buffer solution to demonstrate their propensity for unidirectional assembly. Figure 2a shows that Fmoc-YA and Fmoc-YS can also stabilize chloroform-in-water emulsions. Infrared spectra (Figure 2b) confirm the presence of β sheet-like H-bonding in Fmoc-YL and Fmoc-YA in aqueous media with a much weaker contribution for Fmoc-YS.[58] Figure 2c lists the calculated partition coefficient (log P) and the measured partitioning of peptides between water, chloroform and accumulated at the interface. These values correlate with the critical emulsion concentration (obtained from emulsification experiments as Figure S8 (Supporting Information) shown) of Fmoc-YL, Fmoc-YA and Fmoc-YS and the average diameters of emulsions droplets. It demonstrates that more hydrophobic peptide amphiphiles and stronger H-bonding interactions between the peptide backbones lead to stronger absorption at the chloroform/water interfaces resulting in a decrease in size of emulsion droplets and lower critical emulsion concentrations.

To further increase the hydrophobicity, di- and triphenylalanine were tested as the peptide sequences (Fmoc-FF and Fmoc-FFF). Fmoc-FF was previously demonstrated to form nanofibrous structures.[43,49,59] Figure 2d shows that self-assembled fibers labeled with FITC stabilize the chloroform droplets at the interface. The Fmoc-FFF amphiphiles become too hydrophobic to dissolve in the water phase, but they do dissolve in chloroform. Upon preparation of 10 mM Fmoc-FFF chloroform solution which was added to buffer solution containing FITC and emulsification, the core of the emulsion droplets are fluorescent which indicates the formation of

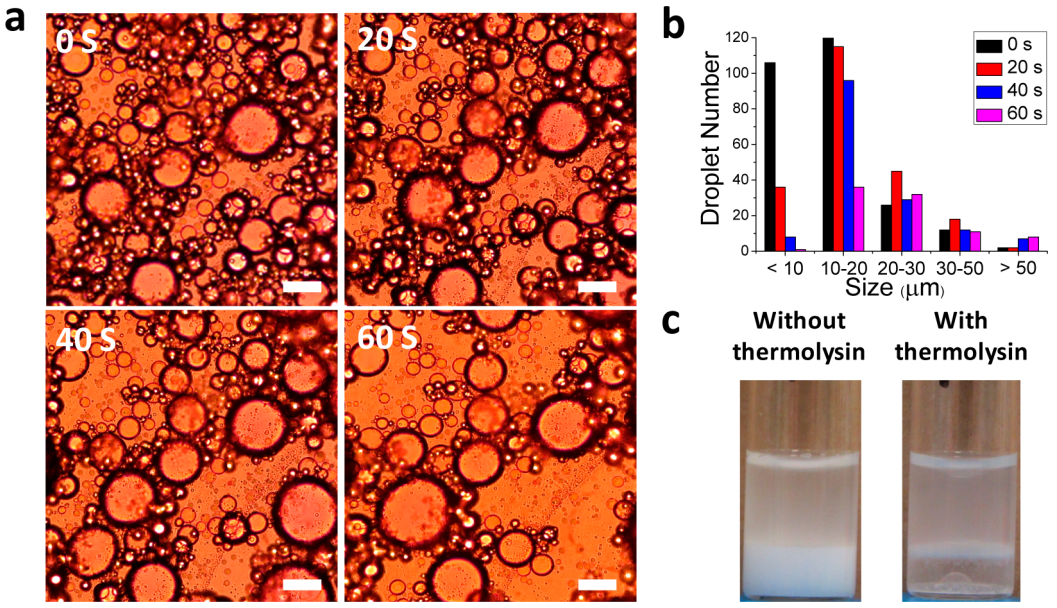

Figure 4. (a) Optical microscope images of adding 1 mg·mL^{-1} thermolysin buffer soultion into chloroform-in-water emulsion droplets stabilized with 2 mmol·L^{-1} Fmoc-YL buffer solution after 0, 20, 40, 60 s. Scale bar is 50 μm. (b) Histogram of the size distribution of adding 1 mg·mL^{-1} thermolysin phosphate buffer solution into chloroform-in-water emulsion droplets stabilized with 2 mmol·L^{-1} Fmoc-YL buffer solution after 0, 20, 40, 60 s. (c) Optical photographs of vials in which emulsions formed (left) and demulsified (right) in addition of thermolysin. Emulsions were stabilized with 2 mmol·L^{-1} Fmoc-YL buffer solution in absence (left) and presence (right) of 1 mg·mL^{-1} thermolysin after 10 min.

water-in-chloroform emulsions (Figure 2e). Replacing the Fmoc group with pyrene, amphiphiles and the emulsion systems are inherently endowed with fluorescent properties. Figure 2f shows the formation of chloroform-in-water emulsion with blue emission stabilized by self-assembly of Pyrene-YL. Clearly, there are opportunities to change the peptide sequences and aromatic moieties further to optimize and functionalize the emulsion systems.

The attraction of using self-assembled barriers of aromatic peptides amphiphiles to stabilize emulsions rather than traditional surfactants, *e.g.*, sodium dodecyl sulfate (SDS), dramatically enhances the stability of emulsions. Figure 3a shows that after 2 weeks at room temperature, the emulsions stabilized by SDS are demulsified and phase-separated, while the emulsions stabilized by Fmoc-YL are still stable. Fmoc-YL stabilized emulsions are heat stable with no visible change observed after exposure to 60 °C for 3 h, which is comparable to the performance of SDS (Figure 3b). In 100 mM phosphate, chloride and thiocyanate solution, 10 mM SDS stabilized emulsions are phase-separated after 24 h as Figure 3c shown, while Fmoc-YL networks are not influenced by the salt effect. Figure S9 (Supporting Information) shows that Fmoc-YL can also stabilize both hexadecane-in-water and mineral oil-in-water emulsions instead of chloroform making the approach general for varied organic media.

Another vital advantage of using peptide self-assembly to stabilize the emulsion systems is the ability to digest the stabilizing film using a suitable enzyme. Proteases, the enzymes that cleave peptide bonds cause disassembly of amphiphiles. Figure 4a and 4b show that after adding thermolysin to Fmoc-YL stabilized emulsions, the emulsion droplets are demulsified and coalesce to bigger droplets in 60 s. When the conversion of cleaving reaction catalyzed by thermolysin in aqueous media reaches 50% detected by high-performance liquid chromatography (HPLC) after 10 min, the complete demulsification and phase separation was observed Figure 4c.

CONCLUSION

In conclusion, we demonstrate the use of aromatic short peptide to self-assemble nanofibrous networks at the organic/aqueous interface to emulsify and stabilize the oil-in-water or water-in-oil emulsions. The formation of peptide microcapsules at interfaces provides long-term and higher stability against temperature and varied salts, compared with traditional surfactant, *e.g.*, SDS. The peptide amphiphiles can be designed by altering aromatic moieties and peptide sequences to manipulate the emulsion stability, droplet size and critical emulsion concentration. The peptide microcapsules can disassemble in the presence of proteolytic enzymes enabling on-demand demulsification under physiological conditions. There are opportunities to expand the molecular design to include fully biocompatible analogues, by replacing the aromatic components with biocompatible ligands, such as nucleotides[60] or using unmodified self-assembling aromatic peptides.[61,62]

The interfacial networks presented here facilitate encapsulation and compartmentalization with potential applications in drug delivery and release, and food industry.

MATERIALS AND METHODS

Materials. Fmoc-Tyr (97%), H-Leu-O*t*Bu·HCl (≥98.0%), Ala-O*t*-Bu·HCl (≥98.0%), *O*-*tert*-Butyl-L-Ser-*tert*-Butyl ester hydrochloride (≥98.0%), *N*,*N*-Diisopropylethylamine (DIPEA) (>99.5%), Trifluoroacetic acid (99%), Sodium hydroxide, 1-Pyreneacetic acid, Fluorescein isothiocyanate isomer I (≥90%), Thioflavin T, Sodium phosphate monobasic monohydrate (ACS reagent, 98.0%−102.0%), Sodium phosphate dibasic heptahydrate (ACS reagent, 98.0%−102.0%), Hexadecane (99%) and Mineral oil were purchased from Sigma-Aldrich and used as received. Fmoc-Phe-Phe-Phe-OH was purchased from BACHEM. 2-(1*H*-Benzotriazole-1-yl)-1,1,3,3-tetramethyluronium hexafluorophosphate (HBTU) was purchased from Novabiochem. Phosphate buffer solution (pH 8) was prepared by dissolving 94 mg of $NaH_2PO_4 \cdot H_2O$ and 2.5 g of $Na_2HPO_4 \cdot 7H_2O$ in 100 mL of water.

Preparation of Emulsions. 10 mM Fmoc-YL solution was prepared by dissolving 5.32 mg of Fmoc-YL in 1 mL of phosphate buffer solution. Different volumes of chloroform were added to Fmoc-YL buffer solution at 80 °C (the volume ratio of buffer solution to chloroform is altered from 1:9, 3:7, 5:5, 7:3, to 9:1, total volume was always 1 mL), after hand-shaking for 5 s emulsions form in vials. For SEM, IR, stability, average particle size, critical emulsion concentration and demulsification measurements, the volume ratio of buffer solution to chloroform was fixed at 7:3. The concentration of all aromatic peptide amphiphiles studied (Fmoc-YA, Fmoc-YS, Pyr-YL, Fmoc-FF and Fmoc-FFF) was 10 mM, except for in the determination of the critical emulsion concentration (0.1−10 mM) and demulsification measurements (2 mM).

Characterization. The structures of Fmoc-YL microcapsules were determined by Hitachi S800 field emission scanning electron microscope (SEM) at an accelerating voltage of 10 keV. The transfer of Fmoc-YL, YA and YS were analyzed by UV−vis spectroscopy (JAS.C.O V-660 spectrophotometer). The formation of Fmoc-YL gels and labeling of ThT were carried out by fluorescence spectroscopy (JAS.C.O FP-6500 spectrofluorometer). High resolution mass spectra (HRMS) were recorded on a Thermo Electron Exactive. 400.1 (1H) NMR spectra were recorded on Bruker Avance 400 spectrometer at room temperature using perdeuterated solvents as internal standards.

The emulsion droplets were characterized by fluorescence microscopy. The devices were mounted on an Epi-fluorescent Upright Microscope (Nikon, Eclipse E600). Images were acquired using Zeiss ×20 dry objective and the appropriate filter set for the fluorophore being imaged. Image was analyzed using ImageJ.

The fibrous structures of Fmoc-YL, YA, YS were determined by atomic force microscopy (AFM). The images were obtained by scanning the mica surface in air under ambient conditions using a Veeco dilNNOVA Scanning Probe Microscope (VEECO/BRUKER, Santa Barbara, CA, USA) operated in tapping mode. 20 μL of solutions were placed on a trimmed and freshly cleaved mica sheet (G250−2 Mica sheets 1″ × 1″ × 0.006″; Agar Scientific Ltd., Essex, UK) attached to an AFM support stub and left to air-dry overnight in a dust-free environment. The AFM scans were taken at 512 × 512 pixels resolution. Typical scanning parameters were as follows: tapping frequency 308 kHz, integral and proportional gains 0.3 and 0.5, respectively, set point 0.5−0.8 V and scanning speed 1.0 Hz.

The β-sheet-like arrangement was determined by infrared absorption spectra, which were recorded on a Bruker Vertex 70 spectrometer, averaging 25 scans per sample at a resolution of 1 cm^{-1}. Samples were sandwiched between two 2 mm CaF_2 windows separated with a 50 μm polytetrafluoroethylene (PTFE) spacer.

Conflict of Interest: The authors declare no competing financial interest.

Acknowledgment. We thank Dr. Margaret Mullin for SEM measurement. The research leading to these results has received funding from the European Research Council under the European Union's Seventh Framework Programme (FP7/2007-2013)/EMERgE/ERC Grant Agreement No. [258775]. The material is based on research sponsored by the Air Force Laboratory, under Agreement Number FA9550-11-1-0263.

Supporting Information Available: Synthesis of peptides, fluorescence spectra of peptide before and after gelation, UV−vis spectra of peptides in water and oil phases, transfer between two phases, AFM images of peptide fibers, and photographs of critical emulsion concentration measurements were showed. This material is available free of charge *via* the Internet at http://pubs.acs.org/.

REFERENCES AND NOTES

1. Pickering, S. U. Emulsions. *J. Chem. Soc.* **1907**, *91*, 2001–2021.
2. Margulies, M.; Egholm, M.; Altman, W. E.; Attiya, S.; Bader, J. S.; Bemben, L. A.; Berka, J.; Braverman, M. S.; Chen, Y. J.; Chen, Z. T.; *et al.* Genome Sequencing in Microfabricated High-Density Picolitre Reactors. *Nature* **2005**, *437*, 376–380.
3. Pearce, K. N.; Kinsella, J. E. Emulsifying Properties of Proteins—Evaluation of A Turbidimetric Technique. *J. Agric. Food Chem.* **1978**, *26*, 716–723.
4. Lochhead, R. Y.; Hemker, W. J.; Castaneda, J. Y. Hydrophobically Modified Carbopol Resins. *Soap, Cosmet., Chem. Spec.* **1987**, *63*, 84.
5. Crossley, S.; Faria, J.; Shen, M.; Resasco, D. E. Solid Nanoparticles That Catalyze Biofuel Upgrade Reactions at the Water/Oil Interface. *Science* **2010**, *327*, 68–72.
6. Muller, R. H.; Mader, K.; Gohla, S. Solid Lipid Nanoparticles (SLN) for Controlled Drug Delivery—A Review of the State of the Art. *Eur. J. Pharm. Biopharm.* **2000**, *50*, 161–177.
7. Chen, L. Y.; Yu, S. Z.; Wang, H.; Xu, J.; Liu, C. C.; Chong, W. H.; Chen, H. Y. General Methodology of Using Oil-in-Water and Water-in-Oil Emulsions for Coiling Nanofilaments. *J. Am. Chem. Soc.* **2013**, *135*, 835–843.
8. Windbergs, M.; Zhao, Y.; Heyman, J.; Weitz, D. A. Biodegradable Core-Shell Carriers for Simultaneous Encapsulation of Synergistic Actives. *J. Am. Chem. Soc.* **2013**, *135*, 7933–7937.
9. Viswanathan, P.; Chirasatitsin, S.; Ngamkham, K.; Engler, A. J.; Battaglia, G. Cell Instructive Microporous Scaffolds through Interface Engineering. *J. Am. Chem. Soc.* **2012**, *134*, 20103–20109.
10. Platzman, I.; Janiesch, J. W.; Spatz, J. P. Synthesis of Nanostructured and Biofunctionalized Water-in-Oil Droplets as Tools for Homing T Cells. *J. Am. Chem. Soc.* **2013**, *135*, 3339–3342.
11. Liu, Y. X.; Jessop, P. G.; Cunningham, M.; Eckert, C. A.; Liotta, C. L. Switchable Surfactants. *Science* **2006**, *313*, 958–960.
12. Ristenpart, W. D.; Bird, J. C.; Belmonte, A.; Dollar, F.; Stone, H. A. Non-Coalescence of Oppositely Charged Drops. *Nature* **2009**, *461*, 377–380.
13. Zhang, J.; Coulston, R. J.; Jones, S. T.; Geng, J.; Scherman, O. A.; Abell, C. One-Step Fabrication of Supramolecular Microcapsules from Microfluidic Droplets. *Science* **2012**, *335*, 690–694.
14. Helgeson, M. E.; Moran, S. E.; An, H. Z.; Doyle, P. S. Mesoporous Organohydrogels from Thermogelling Photocrosslinkable Nanoemulsions. *Nat. Mater.* **2012**, *11*, 344–352.
15. Zhang, W. B.; Zhu, Y. Z.; Liu, X.; Wang, D.; Li, J. Y.; Jiang, L.; Jin, J. Salt-Induced Fabrication of Superhydrophilic and Underwater Superoleophobic PAA-g-PVDF Membranes for Effective Separation of Oil-in-Water Emulsions. *Angew. Chem., Int. Ed.* **2014**, *53*, 856–860.

16. Garcia-Tunon, E.; Barg, S.; Bell, R.; Weaver, J. V. M; Walter, C.; Goyos, L.; Saiz, E. Designing Smart Particles for the Assembly of Complex Macroscopic Structures. *Angew. Chem., Int. Ed.* **2013**, *52*, 7805–7808.
17. Reinhold, S. E.; Desai, K. G. H.; Zhang, L.; Olsen, K. F.; Schwendeman, S. P. Self-Healing Microencapsulation of Biomacromolecules without Organic Solvents. *Angew. Chem., Int. Ed.* **2012**, *51*, 10800–10803.
18. Besnard, L.; Marchal, F.; Paredes, J. F.; Daillant, J.; Pantoustier, N.; Perrin, P.; Guenoun, P. Multiple Emulsions Controlled by Stimuli-Responsive Polymers. *Adv. Mater.* **2013**, *25*, 2844–2848.
19. Villar, G.; Heron, A. J.; Bayley, H. Formation of Droplet Networks that Function in Aqueous Environments. *Nat. Nanotechnol.* **2011**, *6*, 803–808.
20. Hanson, J. A.; Chang, C. B.; Graves, S. M.; Li, Z. B.; Mason, T. G.; Deming, T. J. Nanoscale Double Emulsions Stabilized by Single-Component Block Copolypeptides. *Nature* **2008**, *455*, 85–89.
21. Dexter, A. F.; Malcolm, A. S.; Middelberg, A. P. J. Reversible Active Switching of the Mechanical Properties of a Peptide Film at a Fluid-Fluid Interface. *Nat. Mater.* **2006**, *5*, 502–506.
22. Morikawa, M.; Yoshihara, M.; Endo, T.; Kimizuka, N. Alpha-Helical Polypeptide Microcapsules Formed by Emulsion-Templated Self-Assembly. *Chem.—Eur. J.* **2005**, *11*, 1574–1578.
23. Fletcher, J. M.; Harniman, R. L.; Barnes, F. R. H.; Boyle, A. L.; Collins, A.; Mantell, J.; Sharp, T. H.; Antognozzi, M.; Booth, P. J.; Linden, N.; *et al.* Self-Assembling Cages from Coiled-Coil Peptide Modules. *Science* **2013**, *340*, 595–599.
24. Rozkiewicz, D. I.; Myers, B. D.; Stupp, S. I. Interfacial Self-Assembly of Cell-Like Filamentous Microcapsules. *Angew. Chem., Int. Ed.* **2011**, *50*, 6324–6327.
25. Hermanson, K. D.; Huemmerich, D.; Scheibel, T.; Bausch, A. R. Engineered Microcapsules Fabricated from Reconstituted Spider Silk. *Adv. Mater.* **2007**, *19*, 1810–1815.
26. Wu, C.; Bai, S.; Ansorge-Schumacher, M. B.; Wang, D. Y. Nanoparticle Cages for Enzyme Catalysis in Organic Media. *Adv. Mater.* **2011**, *23*, 5694–5699.
27. Cui, M. M.; Emrick, T.; Russell, T. P. Stabilizing Liquid Drops in Nonequilibrium Shapes by the Interfacial Jamming of Nanoparticles. *Science* **2013**, *342*, 460–463.
28. Miesch, C.; Kosif, I.; Lee, E.; Kim, J. K.; Russell, T. P.; Hayward, R. C.; Emrick, T. Nanoparticle-Stabilized Double Emulsions and Compressed Droplets. *Angew. Chem., Int. Ed.* **2012**, *51*, 145–149.
29. Kosif, I.; Cui, M. M.; Russell, T. P.; Emrick, T. Triggered *In Situ* Disruption and Inversion of Nanoparticle-Stabilized Droplets. *Angew. Chem., Int. Ed.* **2013**, *52*, 6620–6623.
30. Jiang, J. H.; Zhu, Y.; Cui, Z. G.; Binks, B. P. Switchable Pickering Emulsions Stabilized by Silica Nanoparticles Hydrophobized *In Situ* with a Switchable Surfactant. *Angew. Chem., Int. Ed.* **2013**, *52*, 12373–12376.
31. Yang, H. Q.; Zhou, T.; Zhang, W. J. A Strategy for Separating and Recycling Solid Catalysts Based on the pH-Triggered Pickering-Emulsion Inversion. *Angew. Chem., Int. Ed.* **2013**, *52*, 7455–7459.
32. Chen, T.; Colver, P. J.; Bon, S. A. F. Organic-Inorganic Hybrid Hollow Spheres Prepared from TiO_2-Stabilized Pickering Emulsion Polymerization. *Adv. Mater.* **2007**, *19*, 2286–2289.
33. Dinsmore, A. D.; Hsu, M. F.; Nikolaides, M. G.; Marquez, M.; Bausch, A. R.; Weitz, D. A. Colloidosomes: Selectively Permeable Capsules Composed of Colloidal Particles. *Science* **2002**, *298*, 1006–1009.
34. Shum, H. C.; Zhao, Y. J.; Kim, S. H.; Weitz, D. A. Multicompartment Polymersomes from Double Emulsions. *Angew. Chem., Int. Ed.* **2011**, *50*, 1648–1651.
35. Wang, Z.; van Oers, M. C. M.; Rutjes, F. P. J. T.; van Hest, J. C. M. Polymersome Colloidosomes for Enzyme Catalysis in a Biphasic System. *Angew. Chem., Int. Ed.* **2012**, *51*, 10746–10750.
36. Wiese, S.; Spiess, A. C.; Richtering, W. Microgel-Stabilized Smart Emulsions for Biocatalysis. *Angew. Chem., Int. Ed.* **2013**, *52*, 576–579.
37. Adams, D. J.; Topham, P. D. Peptide Conjugate Hydrogelators. *Soft Matter* **2010**, *6*, 3707–3721.
38. Smith, A. M.; Ulijn, R. V. Designing Peptide Based Nanomaterials. *Chem. Soc. Rev.* **2008**, *37*, 664–675.
39. Bowerman, C. J.; Nilsson, B. L. Review Self-Assembly of Amphipathic *beta*-Sheet Peptides: Insights and Applications. *Biopolymers* **2012**, *98*, 169–184.
40. Yan, X. H.; Zhu, P. L.; Li, J. B. Self-Assembly and Application of Diphenylalanine-Based Nanostructures. *Chem. Soc. Rev.* **2010**, *39*, 1877–1890.
41. Raeburn, J.; Alston, B.; Kroeger, J.; McDonald, T. O.; Howse, J. R.; Cameron, P. J.; Adams, D. J. Electrochemically-Triggered Spatially and Temporally Resolved Multi-Component Gels. *Mater. Horiz.* **2014**, *1*, 241–246.
42. Johnson, E. K.; Adams, D. J.; Cameron, P. J. Directed Self-Assembly of Dipeptides to Form Ultrathin Hydrogel Membranes. *J. Am. Chem. Soc.* **2010**, *132*, 5130–5136.
43. Braun, H. G.; Cardoso, A. Z. Self-Assembly of Fmoc-Diphenylalanine inside Liquid Marbles. *Colloids Surf., B* **2012**, *97*, 43–50.
44. Williams, R. J.; Smith, A. M.; Collins, R.; Hodson, N.; Das, A. K.; Ulijn, R. V. Enzyme Assisted Self-Assembly under Thermodynamic Control. *Nat. Nanotechnol.* **2009**, *4*, 19–24.
45. Bai, S.; Debnath, S.; Gibson, K.; Schlicht, B.; Bayne, L.; Zagnoni, M.; Ulijn, R. V. Biocatalytic Self-Assembly of Nanostructured Peptide Microparticles Using Droplet Microfluidics. *Small* **2014**, *10*, 285–293.
46. Mann, S. The Origins of Life: Old Problems, New Chemistries. *Angew. Chem., Int. Ed.* **2013**, *52*, 10746–10750.
47. Zou, Q.; Zhang, L.; Yan, X.; Wang, A.; Ma, G.; Li, J.; Möhwald, H.; Mann, S. Multifunctional Porous Microspheres Based on Peptide-Porphyrin Hierarchical Co-Assembly. *Angew. Chem., Int. Ed.* **2014**, *53*, 2366–2370.
48. Morris, K. L.; Chen, L.; Raeburn, J.; Sellick, O. R.; Cotanda, P.; Paul, A.; Griffiths, P. C.; King, S. M.; O' Reilly, R. K.; Serpell, L. C.; Adams, D. J. Chemically Programmed Self-Sorting of Gelator Networks. *Nat. Commun.* **2013**, *4*, 1480.
49. Mahler, A.; Reches, M.; Rechter, M.; Cohen, S.; Gazit, E. Rigid, Self-Assembled Hydrogel Composed of a Modified Aromatic Dipeptide. *Adv. Mater.* **2006**, *18*, 1365–1370.
50. Hirst, A. R.; Roy, S.; Arora, M.; Das, A. K.; Hodson, N.; Murray, P.; Marshall, S.; Javid, N.; Sefcik, J.; Boekhoven, J.; van Esch, J. H.; Santabarbara, S.; Hunt, N. T.; Ulijn, R. V. Biocatalytic Induction of Supramolecular Order. *Nat. Chem.* **2010**, *2*, 1089–1094.
51. Fleming, S.; Debnath, S.; Frederix, P. W. J. M.; Hunt, N. T.; Ulijn, R. V. Insights into the Co-Assembly of Hydrogelators and Surfactants Based on Aromatic Peptide Amphiphiles. *Biomacromolecules* **2014**, 10.1021/bm240170z.
52. Zhang, Y.; Yang, Z. M.; Yuan, F.; Gu, H. W.; Gao, P.; Xu, B. Molecular Recognition Remolds the Self-Assembly of Hydrogelators and Increases the Elasticity of the Hydrogel by 10(6)-fold. *J. Am. Chem. Soc.* **2004**, *126*, 15028–15029.
53. Yang, J. J.; Van Wart, H. E. Kinetics of Hydrolysis of Dansyl Peptide Substrates by Thermolysin: Analysis of Fluorescence Changes and Determination of Steady-State Kinetic Parameters. *Biochemistry* **1994**, *33*, 6508–6515.
54. Roy, S.; Javid, N.; Frederix, P. W. J. M.; Lamprou, D. A.; Urquhart, A. J.; Hunt, N. T.; Halling, P. J.; Ulijn, R. V. Dramatic Specific-Ion Effect in Supramolecular Hydrogels. *Chem.—Eur. J.* **2012**, *18*, 11723–11731.
55. Roy, S.; Javid, N.; Sefcik, J.; Halling, P. J.; Ulijn, R. V. Salt-Induced Control of Supramolecular Order in Biocatalytic Hydrogelation. *Langmuir* **2012**, *28*, 16664–16670.
56. Gebbink, M. F. B. G.; Claessen, D.; Bouma, B.; Dijkhuizen, L.; Wosten, H. A. B. Amyloids—A Functional Coat for Microorganisms. *Nat. Rev. Microbiol.* **2005**, *3*, 333–341.
57. Fleming, S.; Frederix, P. W. J. M.; Ramos-Sasselli, I.; Hunt, N.; Ulijn, R. V.; Tuttle, T. Assessing the Utility of Infrared Spectroscopy as a Structural Diagnostic Tool for β-sheets in Self-Assembling Aromatic Peptide Amphiphiles. *Langmuir* **2013**, *29*, 9510–9515.
58. Hughes, M.; Birchall, L. S.; Zuberi, K.; Aitkin, L. A.; Debnath, S.; Javid, N.; Ulijn, R. V. Differential Supramolecular Organisation of Fmoc-Dipeptides with Hydrophilic Terminal

Amino Acid Residues by Biocatalytic Self-Assembly. *Soft Matter* **2012**, *8*, 11565–11574.
59. Smith, A. M.; Williams, R. J.; Tang, C.; Coppo, P.; Collins, R. F.; Turner, M. L.; Saiani, A.; Ulijn, R. V. Fmoc-Diphenylalanine Self Assembles to a Hydrogel *via* a Novel Architecture Based on *pi-pi* Interlocked *beta*-Sheets. *Adv. Mater.* **2008**, *20*, 37–41.
60. Li, X.; Kuang, Y.; Lin, H. C.; Gao, Y.; Shi, J.; Xu, B. Supramolecular Nanofibers and Hydrogels of Nucleopeptides. *Angew. Chem., Int. Ed.* **2011**, *50*, 9365–9369.
61. Reches, M.; Gazit, E. Casting Metal Nanowires within Discrete Self-Assembled Peptide Nanotubes. *Science* **2003**, *300*, 625–627.
62. Moitra, P.; Kumar, K.; Kondaiah, P.; Bhattacharya, S. Efficacious Anticancer Drug Delivery Mediated by a pH-Sensitive Self-Assembly of a Conserved Tripeptide Derived from Tyrosine Kinase NGF Receptor. *Angew. Chem., Int. Ed.* **2014**, *53*, 1113–1117.